PRL **105,** 156001 (2010) PHYSICAL REVIEW LETTERS week ending 8 OCTOBER 2010

Active Microrheology: A Proposed Technique to Measure Normal Stress Coefficients of Complex Fluids

Aditya S. Khair and Todd M. Squires
Department of Chemical Engineering, University of California, Santa Barbara, California 93106-5080, USA

(Received 30 May 2010; published 6 October 2010)

We propose a microrheological technique to measure normal stress coefficients (NSCs) of complex fluids, which would represent the first quantitatively accurate measurement of a nonlinear rheological property by microrheology. Specifically, the mechanical response of almost all complex fluids to "weakly nonlinear" deformations is described by the second-order fluid model. Two microrheological probes pulled with equal velocities through a second-order fluid experience a relative force that is linear in the first and second NSCs of the complex fluid. We compute the coupling matrix between NSCs and relative forces for probes translating parallel and perpendicular to their line of centers, which can be inverted to yield NSCs from measured relative forces. There exists an optimum probe separation for inversion of the coupling matrix and, hence, experimental recovery of NSCs.

DOI: 10.1103/PhysRevLett.105.156001 PACS numbers: 83.85.Lq, 47.15.G−, 47.57.−s, 83.60.Hc

Microrheology aims to infer rheological properties of soft materials and complex fluids using colloidal probe particles [1–5]. In *passive*, or Brownian, microrheology, the probe moves randomly due to thermal fluctuations of its surroundings. The probe's mean-squared displacement is measured, from which the linear viscoelastic moduli (or, equivalently, complex viscosity) of the material are calculated via the generalized Stokes-Einstein relation [5,6]. In nonlinear microrheology, the probe is *actively* pulled through the complex fluid, with the aim of driving the material out of equilibrium and measuring nonlinear rheological properties. Crucially, the material's nonequilibrium microstructure renders the generalized Stokes-Einstein relation inapplicable. Nonlinear active microrheology experiments have been performed on suspensions near the glass transition [7], colloidal dispersions [8,9], and DNA solutions [10], while modeling has focused on dilute hard-sphere colloids [11,12] and Brownian dynamics simulations of sphere [13] and rod [14] suspensions. Typically, the force required to maintain the probe at a given velocity is measured (or computed) and recast as a velocity-dependent "microviscosity," by using a generalized Stokes drag. However, this assumed relation between measured probe motion and material rheology is fraught with difficulties and does not, in general, recover true rheological properties [15]. Furthermore, almost all existing techniques are limited to extracting a frequency- or velocity-dependent viscosity, whereas conventional "macrorheological" techniques can, in principle, determine the entire stress tensor [16,17].

In particular, complex fluids often posses normal stress coefficients (NSCs), which are nonlinear material properties that cause visually dramatic and counterintuitive flow phenomena, e.g., "rod climbing" of polymer solutions due to tension along curved streamlines [16], purely elastic instabilities in inertialess viscometric flows [18], and "elastic turbulence" [19]. Formally, in a simple shear flow with velocity $u_x = \dot{\gamma} y$ (with shear rate $\dot{\gamma}$ and flow, gradient, and vorticity directions x, y, and z, respectively), the first and second NSCs are defined as $\Psi_1 = (\tau_{xx} - \tau_{yy})/\dot{\gamma}^2$ and $\Psi_2 = (\tau_{yy} - \tau_{zz})/\dot{\gamma}^2$, respectively, where τ_{ij} are components of the deviatoric stress tensor [16]. Clearly, $\Psi_1 = \Psi_2 = 0$ for a Newtonian fluid. For example, polymer solutions have $\Psi_1 > 0$ and $\Psi_2 < 0$. One can measure Ψ_1 in parallel-plate or cone-and-plate rheometers, as the force acting to drive the rheometer walls apart is directly proportional to it. Simultaneous measurement of Ψ_1 and Ψ_2 is significantly more challenging, requiring rheo-optical methods [20] or a modified cone-and-plate apparatus with pressure transducers fitted along the plate [21].

Here, we present a novel technique to measure NSCs by active microrheology, which would represent the first unambiguous and quantitatively accurate microrheological measurement of a nonlinear rheological quantity. Specifically, we propose to pull two identical torque-free spherical colloidal probes with equal velocities through a complex fluid and measure the relative force F_R between them. At very small pulling speeds U, the fluid microstructure recovers instantaneously from the probe motion, and the hydrodynamic stress on the probes is linear in U and Newtonian in form. In this case, F_R is identically zero, as a consequence of reversibility and symmetry at zero Reynolds number [22]. For pulling speeds sufficiently large to drive the microstructure just "weakly" out of equilibrium, the stress becomes non-Newtonian and nonlinear in U, resulting in a nonzero F_R. In this "weakly nonlinear" regime, the deviatoric stress $\boldsymbol{\tau}$ for almost all complex fluids can be represented by the second-order fluid model [16]

$$\boldsymbol{\tau} = \eta \boldsymbol{A}_{(1)} - \tfrac{1}{2}\Psi_1 \boldsymbol{A}_{(2)} + \Psi_2 \boldsymbol{A}_{(1)} \cdot \boldsymbol{A}_{(1)}, \qquad (1)$$

where η is the shear viscosity and $\boldsymbol{A}_{(1)} = \boldsymbol{\nabla u} + (\boldsymbol{\nabla u})^T$ and $\boldsymbol{A}_{(2)} = D\boldsymbol{A}_{(1)}/Dt - (\boldsymbol{\nabla u})^T \cdot \boldsymbol{A}_{(1)} - \boldsymbol{A}_{(1)} \cdot \boldsymbol{\nabla u}$ are the first and second Rivlin-Ericksen tensors, respectively, with $\boldsymbol{\nabla u}$ the velocity gradient tensor. The second-order fluid captures the "first" non-Newtonian material response with increasing flow speed. The first term in (1) is simply the Newtonian stress; the remaining terms are non-Newtonian stresses, which are proportional to the NSCs and scale as velocity squared. Hence, the relative force F_R acting on the probes is linearly dependent on the NSCs and proportional to the square of their velocities. Since Ψ_1 and Ψ_2 are two unknown quantities to be determined, we require two independent measurements of F_R. An intuitive choice is to pull the probes parallel and perpendicular to their line of centers. The relative forces in each case, $F_R^{\|}$ and $F_R^{\perp}$, are then related to the NSCs via

$$\begin{pmatrix} F_R^{\|} \\ F_R^{\perp} \end{pmatrix} = \begin{pmatrix} C_1^{\|} & C_2^{\|} \\ C_1^{\perp} & C_2^{\perp} \end{pmatrix} \begin{pmatrix} \Psi_1 \\ \Psi_2 \end{pmatrix} U^2. \tag{2}$$

In the dimensional equation above, the elements $C_i^{\|}$ and $C_i^{\perp}$ ($i = 1, 2$) of the "coupling matrix" $\mathcal{C}$ are dimensionless functions of the scaled probe separation d/a only (the probes have radii a and are separated by $2d$). To obtain the matrix elements requires an explicit calculation of the relative force between the probes as they are pulled through a second-order fluid. Once $\mathcal{C}$ has been obtained, (2) can be inverted to determine Ψ_1 and Ψ_2 from an experimental measurement of the relative forces $F_R^{\|}$ and $F_R^{\perp}$ at a prescribed U. Significantly, $\mathcal{C}$ is *independent* of the non-Newtonian properties of a specific fluid, which are contained in Ψ_1 and Ψ_2. Thus, our technique enables microrheological measurement of NSCs for all complex fluids that behave as second-order fluids under weakly nonlinear deformations.

Computing the matrix elements for arbitrary separations is challenging. It is, therefore, tempting to consider widely separated probes $d/a \gg 1$, for which asymptotic techniques are applicable. Indeed, Brunn [23] used the method of reflections to obtain $C_1^{\|} = C_1^{\perp} = \frac{9\pi}{4}(\frac{a}{d})^2$ and $C_2^{\|} = C_2^{\perp} = \frac{9\pi}{8}(\frac{a}{d})^2$. However, using these values with (2) we find the matrix is singular and thus cannot be inverted. This implies that $F_R^{\|}$ and $F_R^{\perp}$ are not linearly independent for $d/a \gg 1$, necessitating computation of the relative forces at arbitrary separations.

Conservation of momentum requires that the total stress in the fluid $\boldsymbol{\sigma}$ satisfies $\boldsymbol{\nabla} \cdot \boldsymbol{\sigma} = 0$, where $\boldsymbol{\sigma} = -p\boldsymbol{I} + \boldsymbol{\tau}$ and p is the dynamic pressure. Additionally, the fluid is incompressible ($\boldsymbol{\nabla} \cdot \boldsymbol{u} = 0$). Henceforth, we employ dimensionless variables with distance, velocity, and stress scaled by a, U, and $\eta U/a$, respectively. We invoke the weakly nonlinear limit by expanding the velocity and pressure as $\{\boldsymbol{u}, p\} = \{\boldsymbol{u}_0, p_0\} + \mathrm{De}\{\boldsymbol{u}_1, p_1\} + O(\mathrm{De}^2)$, where the Deborah number $\mathrm{De} = t_r/t_f$ is the ratio of relaxation t_r to flow t_f time scales. The momentum equation then yields $\boldsymbol{\nabla} \cdot \boldsymbol{\sigma}_0 = \boldsymbol{\nabla} \cdot \boldsymbol{\sigma}_1 = 0$, where

$$\boldsymbol{\sigma}_0 = -p_0\boldsymbol{I} + \boldsymbol{A}_{(1)0}, \tag{3}$$

$$\boldsymbol{\sigma}_1 = -p_1\boldsymbol{I} + \boldsymbol{A}_{(1)1} - \boldsymbol{A}_{(2)0} - B\boldsymbol{A}_{(1)0} \cdot \boldsymbol{A}_{(1)0}, \tag{4}$$

along with continuity $\boldsymbol{\nabla} \cdot \boldsymbol{u}_0 = \boldsymbol{\nabla} \cdot \boldsymbol{u}_1 = 0$. Here, $B = -2\Psi_2/\Psi_1$. At $O(\mathrm{De}^0)$ the fluid motion satisfies the homogeneous Stokes equation, and the relative force is identically zero. Non-Newtonian effects appear at $O(\mathrm{De})$, as a "non-Newtonian body force" $\boldsymbol{\nabla} \cdot (\boldsymbol{A}_{(2)0} + B\boldsymbol{A}_{(1)0} \cdot \boldsymbol{A}_{(1)0})$ originating from gradients in the *Newtonian* velocity field.

In principle, obtaining the $O(\mathrm{De})$ velocity and pressure fields requires solving the inhomogeneous Stokes (partial differential) equations around two spheres—a tedious task. Remarkably, however, one does not need these detailed flow fields to compute the $O(\mathrm{De})$ relative forces. Instead, the Lorentz reciprocal theorem provides a convenient route to determine the forces on particles in weakly viscoelastic [24] (or inertial [25]) flows. Let $\boldsymbol{\sigma}_{\mathrm{aux}}$ and $\boldsymbol{u}_{\mathrm{aux}}$ be the stress and velocity fields, respectively, of an auxiliary Stokes flow around two spherical probes. Then, it is clearly true that

$$\int_{V_f} [\boldsymbol{u}_{\mathrm{aux}} \cdot (\boldsymbol{\nabla} \cdot \boldsymbol{\sigma}_1) - \boldsymbol{u}_1 \cdot (\boldsymbol{\nabla} \cdot \boldsymbol{\sigma}_{\mathrm{aux}})] dV_f = 0, \tag{5}$$

where the integral is over the entire fluid volume. Following Phillips [26], one can show from (5) that

$$\begin{aligned} &\boldsymbol{U}_{\mathrm{aux}}^1 \cdot \boldsymbol{F}^1 + \boldsymbol{U}_{\mathrm{aux}}^2 \cdot \boldsymbol{F}^2 + \boldsymbol{\Omega}_{\mathrm{aux}}^1 \cdot \boldsymbol{L}^1 + \boldsymbol{\Omega}_{\mathrm{aux}}^2 \cdot \boldsymbol{L}^2 \\ &\quad = -\int_{V_f} (\boldsymbol{A}_{(2)0} + B\boldsymbol{A}_{(1)0} \cdot \boldsymbol{A}_{(1)0}) : \boldsymbol{\nabla u}_{\mathrm{aux}} dV_f, \end{aligned} \tag{6}$$

where the superscripts 1 and 2 refer to each probe, $\boldsymbol{U}_{\mathrm{aux}}^i$ and $\boldsymbol{\Omega}_{\mathrm{aux}}^i$ ($i = 1, 2$) are the imposed translational and angular velocities, respectively, on the probes in the auxiliary problem, and $\boldsymbol{F}^i$ and $\boldsymbol{L}^i$ are the $O(\mathrm{De})$ forces and torques, respectively, on the probes in the second-order fluid. To obtain the relative force F_R we choose the auxiliary flow to be that around two probes translating toward each other with velocities $\boldsymbol{U}_{\mathrm{aux}}^1 = -\boldsymbol{U}_{\mathrm{aux}}^2 = -\hat{\boldsymbol{U}}_{\mathrm{aux}}$ (with $\hat{\boldsymbol{U}}_{\mathrm{aux}}$ a unit vector). Hence, $F_R = \hat{\boldsymbol{U}}_{\mathrm{aux}} \cdot (\boldsymbol{F}^1 - \boldsymbol{F}^2)$ and from (6)

$$F_R = \int_{V_f} (\boldsymbol{A}_{(2)0} + B\boldsymbol{A}_{(1)0} \cdot \boldsymbol{A}_{(1)0}) : \boldsymbol{\nabla u}_{\mathrm{aux}} dV_f. \tag{7}$$

Thus, the reciprocal theorem enables the non-Newtonian $O(\mathrm{De})$ relative force F_R to be expressed as the volume integral of quantities that depend only on the Newtonian $O(\mathrm{De}^0)$ flow, contracted with the gradient of the auxiliary Stokes flow $\boldsymbol{u}_{\mathrm{aux}}$. Specifically, with (2) we find

$$C_1 = -\frac{1}{2} \int_{V_f} \boldsymbol{A}_{(2)0} : \boldsymbol{\nabla u}_{\mathrm{aux}} dV_f, \tag{8}$$

$$C_2 = \int_{V_f} (\boldsymbol{A}_{(1)0} \cdot \boldsymbol{A}_{(1)0}) : \boldsymbol{\nabla u}_{\mathrm{aux}} dV_f, \tag{9}$$

which are valid for either parallel or perpendicular probe-pair translation and precisely correspond to the matrix elements in (2). Notably, only the Newtonian $O(\mathrm{De}^0)$

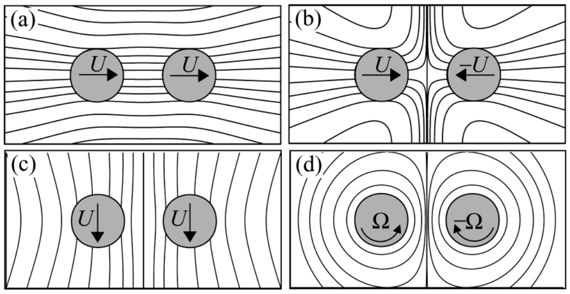

FIG. 1. The four Newtonian $O(\mathrm{De}^0)$ flow fields used to compute non-Newtonian $O(\mathrm{De})$ relative forces between two spherical probes via the reciprocal theorem: (a) parallel translation with equal velocities U [27]; (b) the "auxiliary" flow around probes translating toward one other [29]; (c) translation of nonrotating probes; and (d) counterrotating probes that do not translate. The velocity field for perpendicular translation of freely rotating probes is a combination of (c) and (d), where the angular velocity Ω in (d) is chosen such that the torque on each probe in the composite "(c) + (d)" flow is zero [28]. Here, $d/a = 1.75$ corresponding to the minimum in the coupling matrix condition number (Fig. 4).

velocity fields for parallel and perpendicular translation are required, along with the auxiliary flow (Fig. 1). For parallel translation, the velocity field is axisymmetric and thus can be represented as derivatives of a stream function that satisfies the biharmonic equation [27]. The velocity field for perpendicular translation is three-dimensional; however, each velocity component can be written as the sum of bispherical eigenfunctions of the Stokes equations [28]. Last, the auxiliary flow is axisymmetric, allowing again for a stream function representation [29]. Since each flow is represented in bispherical coordinates, we perform the quadrature in (8) and (9) by using this coordinate system; the integrands scale as R^{-6} for large distances R and are hence absolutely convergent.

Figures 2 and 3 plot the parallel $C_i^{\|}$ and perpendicular $C_i^{\perp}$ matrix elements, respectively, versus probe separation d/a. There is no critical separation where F_R switches sign, since these elements do not change sign at any d/a. Hence, the nature of the relative force (repulsive or attractive) is determined solely by the values of Ψ_1 and Ψ_2. Ardekani, Rangel, and Joseph [30] computed $C_i^{\|}$ and $C_i^{\perp}$ for the sole case of $\Psi_1 = -2\Psi_2$ using the bispherical flow solutions [27,28]. Our results are not subject to this stringent restriction and are therefore significantly more general. Phillips [26] considered the mobility problem of probes subject to equal external forces and obtained the equivalent matrix elements for $d/a > 3$ using a multipole expansion. Our technique requires the resistance problem of translation with equal velocities. The resistance and mobility matrix elements are not generally equal, except as $d/a \to \infty$.

The coupling matrix $\mathcal{C}$ is invertible at all finite separations. Thus, NSCs can be recovered quantitatively from measured relative forces. Experimentally, widely separated probes are clearly undesirable, as $\mathcal{C}$ becomes singular as $d/a \to \infty$. Here, even small errors in measured relative forces yield large errors in inferred NSCs. Indeed, the optimal separation for such an experiment is that for which Ψ_1 and Ψ_2 are least sensitive to errors in F_R. A precise metric of this sensitivity is provided by the matrix condition number κ: The smaller the value of κ, the less influence measurement errors in relative forces have on NSCs. In the Euclidean norm, $\kappa = \sqrt{\rho_{\max}/\rho_{\min}}$, where $\rho_{\max}$ and $\rho_{\min}$ are the maximum and minimum singular values of $\mathcal{C}$, respectively. Hence, the minimum κ can attain is unity (in any matrix norm). Figure 4 shows that κ does not monotonically decrease as the probes are brought closer. Instead, it attains a minimum value at $d/a \approx 1.75$, representing the optimal separation for experiments, at which Ψ_1 and Ψ_2 are least sensitive to errors in F_R. Moreover, parallel $\|$ and perpendicular $\perp$ translations are the optimal pair of directions; it can be shown that translation at any other angle relative to the line of centers gives a higher κ.

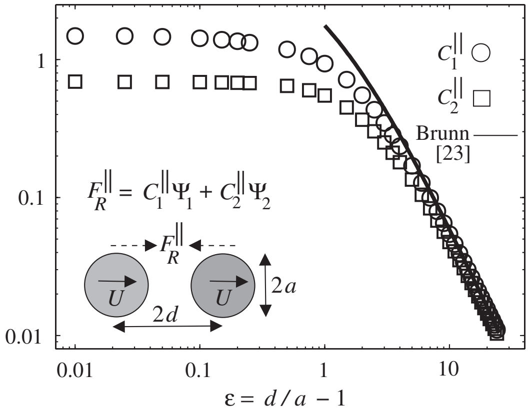

FIG. 2. Matrix coefficients $C_1^{\|}$ and $C_2^{\|}$ versus probe separation $\epsilon = d/a - 1$ for translation along line of centers.

Last, we comment on the potential experimental realizations of our technique. A possible setup involves holding

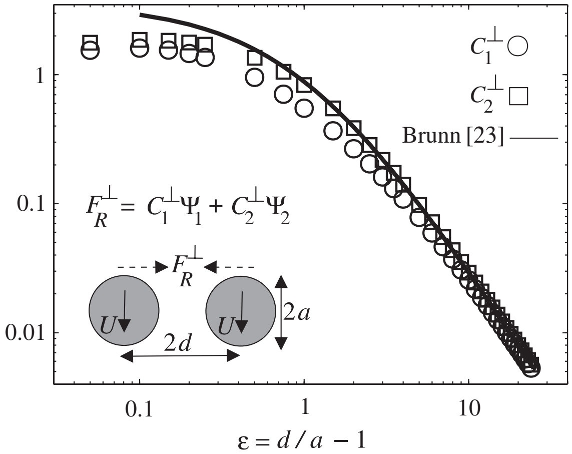

FIG. 3. Matrix coefficients $C_1^{\perp}$ and $C_2^{\perp}$ versus probe separation $\epsilon = d/a - 1$ for translation perpendicular to line of centers.

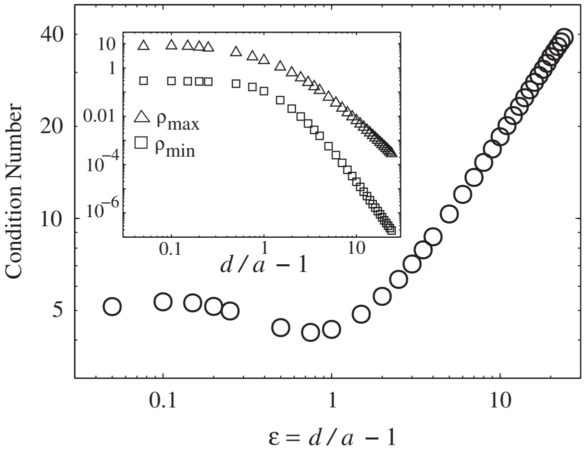

FIG. 4. Condition number $\kappa = \sqrt{\rho_{\max}/\rho_{\min}}$ of the coupling matrix $\mathcal{C}$. The inset shows the maximum $\rho_{\max}$ and minimum $\rho_{\min}$ singular values.

the two probes at a fixed separation in a dual optical trap, as a stage containing the complex fluid is translated past them with speed U_{stg}. The trapping force on each probe is measured, and the difference between forces equals the relative force F_R due to non-Newtonian fluid flow. In the second-order-fluid limit ($\text{De} < 1$), $F_R \sim U_{\text{stg}}^2$. At larger De, F_R is expected to be a more complicated function of U_{stg}, owing to stronger nonlinear effects such as a shear-rate-dependent viscosity. Hence, F_R can be measured for increasing U_{stg}, and the region over which F_R/U_{stg}^2 is constant is where our proposed technique is valid.

For probes of radius $a = 1\ \mu\text{m}$, the trapping force in optical tweezers is of the order of $F_{\text{trap}} \approx 0.1$–$10$ pN [8]. Hence, for $U_{\text{stg}} \approx 10$–$1000\ \mu\text{m/s}$, to first hold the probes against Stokes drag sets a viscosity window of $\eta = F_{\text{trap}}/6\pi a U_{\text{stg}} \approx 0.01$–$50\ \text{mPa}\cdot\text{s}$. Furthermore, F_{trap} prevents relative motion due to NSCs for $\Psi_1, \Psi_2 \sim F_{\text{trap}}/U_{\text{stg}}^2 \approx 0.0001$–$100\ \text{mPa}\cdot\text{s}^2$. This last range is too low to be accessed by almost all existing methods; thus, our technique may offer a highly sensitive measurement of NSCs.

Our technique is applicable to colloidal dispersions. Scaling arguments yield $\Psi_1, \Psi_2 \sim \phi^2 \eta \text{De}/\dot{\gamma}$ for dilute hard-sphere dispersions at small De [31]. Here, ϕ is the (small) volume fraction of "bath" colloids and $\text{De} = t_r/t_f = (b^2/D)/(a/U_{\text{stg}})$, where b and D are the radius and diffusivity of a bath colloid, respectively, and $\dot{\gamma} = U_{\text{stg}}/a$. By using reasonable experimental values of $\eta = 10\ \text{mPa}\cdot\text{s}$, $b = 0.1\ \mu\text{m}$, and $\phi = 0.1$ [8,9], $U_{\text{stg}} < 20\ \mu\text{m/s}$ is required to maintain $\text{De} < 1$, within the range of accessible stage speeds. Further, $\Psi_1, \Psi_2 \approx 0.005\ \text{mPa}\cdot\text{s}^2$ for $U_{\text{stg}} = 20\ \mu\text{m/s}$; hence, the NSCs are within the measurable range from above. We anticipate that our technique can measure NSCs of other complex fluids in which probes can be optically trapped, such as polymer or wormlike micelle solutions. Therefore, we expect the present work to spur a new experimental thrust in nonlinear microrheology and, importantly, allow for a quantitatively accurate microrheological measurement of a nonlinear rheological property.

We gratefully acknowledge the NSF for support under CBET-730270 and E. Furst for discussion and collaboration.

[1] T. G. Mason and D. A. Weitz, Phys. Rev. Lett. **74**, 1250 (1995).
[2] T. G. Mason *et al.*, Phys. Rev. Lett. **79**, 3282 (1997).
[3] F. Gittes *et al.*, Phys. Rev. Lett. **79**, 3286 (1997).
[4] M. L. Gardel and D. A. Weitz, in *Microscale Diagnostic Techniques*, edited by K. Breuer (Springer, Berlin, 2005).
[5] T. M. Squires and T. G. Mason, Annu. Rev. Fluid Mech. **42**, 413 (2010).
[6] T. G. Mason, Rheol. Acta **39**, 371 (2000).
[7] P. Habdas *et al.*, Europhys. Lett. **67**, 477 (2004).
[8] A. Meyer *et al.*, J. Rheol. **50**, 77 (2006).
[9] L. G. Wilson *et al.*, J. Phys. Chem. B **113**, 3806 (2009).
[10] C. Gutsche *et al.*, J. Chem. Phys. **129**, 084902 (2008).
[11] T. M. Squires and J. F. Brady, Phys. Fluids **17**, 073101 (2005).
[12] A. S. Khair and J. F. Brady, J. Fluid Mech. **557**, 73 (2006).
[13] I. C. Carpen and J. F. Brady, J. Rheol. **49**, 1483 (2005).
[14] H. H. Wensink and Löwen, Phys. Rev. Lett. **97**, 038303 (2006).
[15] T. M. Squires, Langmuir **24**, 1147 (2008).
[16] R. B. Bird, R. C. Armstrong, and O. Hassager, *Fluid Mechanics*, Dynamics of Polymeric Liquids Vol. 1 (Wiley, New York, 1987).
[17] R. G. Larson, *The Structure and Rheology of Complex Fluids* (Oxford University Press, New York, 1999).
[18] E. S. G. Shaqfeh, Annu. Rev. Fluid Mech. **28**, 129 (1996).
[19] A. Groisman and V. Steinberg, Nature (London) **405**, 53 (2000).
[20] A. Kulkarni, S. Kharchenko, and R. M. Kannan, Rheol. Acta **45**, 951 (2006).
[21] S-G. Baek and J. J. Magda, J. Rheol. **47**, 1249 (2003).
[22] E. M. Purcell, Am. J. Phys. **45**, 3 (1977).
[23] P. Brunn, Rheol. Acta **16**, 461 (1977).
[24] B. P. Ho and L. G. Leal, J. Fluid Mech. **76**, 783 (1976).
[25] R. G. Cox and H. Brenner, Chem. Eng. Sci. **23**, 147 (1968).
[26] R. J. Phillips, J. Fluid Mech. **315**, 345 (1996).
[27] M. Stimson and G. B. Jeffery, Proc. R. Soc. A **111**, 110 (1926).
[28] A. J. Goldman, R. G. Cox, and H. Brenner, Chem. Eng. Sci. **21**, 1151 (1966).
[29] H. Brenner, Chem. Eng. Sci. **16**, 242 (1961).
[30] A. M. Ardekani, R. H. Rangel, and D. D. Joseph, Phys. Fluids **20**, 063101 (2008).
[31] J. F. Brady and M. Vicic, J. Rheol. **39**, 545 (1995).